

Terrestrial cosmogenic-nuclide production systematics calculated from numerical simulations

Jozef Masarik¹, Robert C. Reedy^{*}

Astrophysics and Radiation Measurements Group, Mail Stop D436, Los Alamos National Laboratory, Los Alamos, NM 87545, USA

Received 2 December 1994; accepted 29 August 1995

Abstract

Calculations for the production of cosmogenic nuclides in the Earth's atmospheric and in-situ in the surface are reported and discussed. We calculated production rates of ^3H , ^7Be , ^{10}Be , ^{14}C , and ^{36}Cl in the atmosphere by both galactic cosmic rays and solar protons, and our calculated production rates for ^{14}C agree well with previous results. Production of atmospheric ^7Be and ^{36}Cl by solar protons in polar regions is not negligible. Our production rates and depth dependences for in-situ ^3He , ^{10}Be , ^{14}C , ^{21}Ne , ^{26}Al , and ^{36}Cl agree well with experimental measurements for certain minerals in surface samples. The altitude dependence of in-situ production rates was also calculated.

1. Introduction

The interactions of cosmic-ray particles with the Earth's atmosphere produce a cascade of secondary particles and many cosmic-ray-produced (cosmogenic) nuclides. Many secondaries have enough energy to undergo further collisions and to produce the next generation of secondary particles. Some of the particles produced in this cascade can reach the Earth's surface and induce nuclear reactions in which some cosmogenic nuclides are produced. Near the Earth's surface, the neutron contribution to the production of cosmogenic nuclides is dominant. These nuclear effects of cosmic rays are observable to great

depths, up to $\sim 10^6 \text{ g cm}^{-2}$, due to the decay of charged π -mesons in the Earth's atmosphere giving rise to penetrating muons. The cosmogenic-nuclide concentration in a terrestrial sample depends on the sample's composition, altitude, geomagnetic latitude, and on the manner in which the exposure geometry of the sample has changed with time.

Because of atmospheric shielding, the rates of production of cosmogenic nuclides in terrestrial rocks are far lower than the corresponding rates in meteorites in space, in the lunar surface, or in the Earth's upper atmosphere [1]. However, accelerator mass spectrometry (AMS) for radionuclides have made it possible in recent years to measure very-low concentrations of long-lived cosmogenic radionuclides such as 5.730-yr ^{14}C , 0.3-Ma ^{36}Cl , 0.7-Ma ^{26}Al and 1.5-Ma ^{10}Be . Improvements in conventional mass spectrometry for stable noble-gas isotopes (e.g., [2]) allow us to measure a few rare stable isotopes, such as ^3He

^{*} Corresponding author; E-mail: reedy@lanl.gov.

¹ Max-Planck-Institut für Chemie, Postfach 3060, D-55020 Mainz, Germany.

and ^{21}Ne , made in situ in certain surface materials. The ability to make precise, high-sensitivity measurements of these nuclides in terrestrial rocks has now made it possible to conduct quantitative geochronological and geomorphological studies on time scales of $\sim 10^3$ – 10^7 years [1,2].

The status of production rates for terrestrial in-situ cosmogenic nuclides has recently been reviewed [3]. Many production rates have been measured, but little work has been done on theoretical modeling of such production rates. We report here on numerical simulations for calculating the production rates of terrestrial cosmogenic nuclides. Some work has been done previously on calculating production rates of cosmogenic nuclides in the Earth's atmosphere, but very little has been done on calculating production rates in the Earth's surface. We calculated production rates of cosmogenic nuclides in the Earth's atmosphere as a test of our codes and to check and extend earlier calculations.

Although the general features of cosmic-ray particles in the Earth are fairly well known [1,4], it is difficult to calculate nuclide production rates because of uncertainties in the fluxes of cosmic-ray particles, especially in the Earth's surface, and the lack of cross sections for the production of different nuclei from the target elements of interest. We used a series of codes that have been well tested for the production of cosmogenic nuclides in extraterrestrial matter.

This paper describes in detail calculations of cosmogenic-nuclide production in the Earth's atmosphere and surface based on the LAHET Code System (LCS) for production by galactic-cosmic-ray particles and the Reedy-Arnold model [5] for solar energetic protons (also called solar cosmic rays). LCS is a system of codes that uses only basic physical quantities and principles, without including any free parameters, to numerically simulate all processes relevant in particle production and transport. LCS has previously been tested with cosmogenic-nuclide production in meteorites (e.g., [6]) and in the lunar surface (e.g., [7]). All the tests show good agreement between experimental data and calculations, which confirms the validity of this model. There have been many different models used to calculate production rates of terrestrial cosmogenic nuclides by galactic-cosmic-ray (GCR) particles. The other approaches used to determine production rates

are varied, and it is often hard to determine the causes of differences among the production rates calculated by various models. Unlike our model, most of the other models used for determining the production rates of terrestrial cosmogenic nuclides have not been extensively tested with measurements in extraterrestrial matter. The model in Reedy and Arnold [5] for the production of nuclides by solar energetic particles has also been well tested (e.g., [8]).

2. Calculational models

2.1. Model for GCR particle production and transport

Our model for the simulation of the interaction of primary and secondary GCR particles with matter is based on the LAHET Code System (LCS) [9], which is a system of general-purpose Monte Carlo computer codes (mainly LAHET [9] and MCNP [10]) that treats the relevant physical processes of particle production and transport. In these codes, incident primary particles are transported through matter considering atomic (mainly ionization energy losses) and nuclear interactions. In these nuclear interactions, new (secondary) particles are produced and subsequently transported with their interactions modeled. The LAHET (Los Alamos High Energy Transport) code transports and models the interactions of all charged particles (protons, alpha particles, pions, and muons) and neutrons with energies greater than 15 eV. Neutrons produced with energies less than 15 MeV by the interactions modeled by LAHET are transported and have their interactions calculated with the MCNP (Monte Carlo N-Particle) code, which was designed for such neutron calculations. The LAHET code models nuclear interactions using parameters designed for all nuclei (global parameters) while MCNP uses a library of evaluated cross sections for each neutron reaction. These codes have been frequently tested for a large variety of applications. More details on LCS and its application to cosmic-ray interactions in matter are in [6].

The nature of high-energy particle interactions with matter is to a large extent determined by the

type and energy of the incoming particle. In our LCS calculations, incoming primary particles in the energy range from 10 MeV to 20 GeV are considered. The characteristic feature of interactions at these energies is the production of secondary particles, many of which have enough energy to undergo further collisions in extended targets and contribute to the development of a particle cascade. The type of incident particle determines the character of the cascade process. As cosmic rays consist mainly of strongly-interacting protons and alpha particles, a so-called hadronic cascade (composed of protons, neutrons, pions and other strongly-interacting particles) is produced. This cascade is usually accompanied by an electromagnetic cascade (composed of weakly-interacting particles such as electrons, positrons, muons, photons and neutrinos), which is usually unimportant in the production of nuclides in matter except at great depths. Both of these cascades are called internuclear because in their development particles produced in collisions of the incoming particle with one nucleus interact with other nuclei.

Another type of cascade is the intranuclear cascade. The intranuclear cascade-evaporation model is often used for the description of hadron–nucleus collisions at high energies. An incoming hadron at high energies can be regarded as interacting separately with each of the nucleons within a nucleus, on the basis of very slightly modified single-particle kinematics. All the reaction products of such collisions are assumed to behave in the same way until all have left the nucleus, contributing to the development of the above-mentioned internuclear cascade, or until they reach an energy that is too low for further interactions. After the intranuclear collision, the nucleus still can be excited and some additional particles can be emitted from the nucleus.

LCS uses random numbers and basic nuclear data to model the interactions of particles with matter. The energy and direction of the incident particle that starts each cascade are selected from a specified distribution (see Section 2.2) using random numbers. The location where this incident particle interacts with a nucleus is then randomly selected considering both ionization energy losses along its path and the nature of the reactions that it can make with the various target nuclei. An intranuclear cascade of the particle within the target nucleus is then simulated.

After a preequilibrium calculation is used to further de-excite the nucleus, the nucleus completely “cools” using an evaporation model. The emitted secondary particles are subsequently followed. The particles in the internuclear cascade are recorded to get their fluxes in the specified regions of the target. A sufficient number of incident particles is used to get good statistics for the calculated particle fluxes.

2.2. Galactic-cosmic-ray particle fluxes

The primary cosmic-ray flux at the Earth’s orbit has two components: galactic and solar. As solar-cosmic-ray (SCR) particles have low energies and therefore induce interactions only in a few outermost g cm⁻² of the Earth’s atmosphere, we considered mainly galactic-cosmic-ray (GCR) particles in our calculations. The GCR particles are a mixture of energetic protons (~ 87%), alpha particles (~ 12%), and some heavier nuclei (~ 1%). The spectral distributions of heavier particles are quite similar to the distribution of protons if energy is taken per nucleon. The differences in cross sections for neutron and proton emission in reactions of primary GCR protons and alpha particles are also very small, and therefore we simulated only the propagation of primary protons in the Earth’s atmosphere and surface. The contributions of alpha (and heavier) particles were simply included in the final results by multiplying the proton calculations by a scaling factor, which was found to be 1.4 [6].

The flux of primary GCR particles varies over time. Solar modulation is the dominant source of the observed variability. Therefore we took the primary GCR proton spectrum in the form that accounts for this influence, with a modulation parameter ϕ [11]. We have used this expression elsewhere [6,12] for calculations involving GCR particles. In these calculations, the model Earth was irradiated by a homogeneous and isotropic flux. In most of our calculations we used only one value of the modulation parameter, $\phi = 550$ MeV, which is very close to a long-term average [12], and the effective flux of protons above 10 MeV was 4.56 protons cm⁻² s⁻¹. This effective proton flux was determined from the fitting of lunar experimental data [7] and was used for high ($\geq 60^\circ$) geomagnetic latitudes. In several calculations, we used modulation parameters that correspond to the

minimum in solar activity ($\phi = 375$ MeV), when the intensity of GCR particles is the largest, and to solar maximum ($\phi = 950$ MeV) [12].

2.3. Model of earth's geometry and chemical composition

For these calculations, the Earth was modelled as a sphere with a radius of 6378 km and a surface density of 2 g cm^{-3} . The elemental composition of the surface was assumed to be an average terrestrial one (in weight percents, 0.2% H, 47.3% O, 2.5% Na, 4.0% Mg, 6.0% Al, 29.0% Si, 5.0% Ca, and 6.0% Fe). Except for very high contents of H, changes in this surface composition, or the addition of other elements such as K, have very little effect on the calculated results. To examine the depth dependence of particle fluxes, the sphere near the surface was divided into spherical shells with thicknesses of 5 g cm^{-2} . The fluxes of protons and neutrons within each shell were calculated.

The Earth's atmosphere was modelled as a spherical shell with an inner radius 6378 km and a thickness of 100 km. Its elemental composition (in weight percents) was 75.5% N, 23.2% O, and 1.3% Ar. The atmospheric shell was divided into 29 subshells to account for change in the atmospheric density and temperature and also in order to examine the depth dependence of particle fluxes in the atmosphere. The atmospheric density and the temperature structure of the atmosphere were in accordance with the U.S. Standard Atmosphere, 1976, model [13]. The total thickness of the atmosphere was 1033 g cm^{-2} .

Statistical errors of neutron fluxes calculated using this geometrical model and running 10,000,000 primary GCR protons were at the level of 8–10% for the Earth's surface and on the level of 4–6% for the atmosphere. Statistical errors of the proton fluxes were substantially higher, but as the magnitudes of the proton fluxes are on the level of a few percent of the neutron fluxes, their uncertainties are not significant in the final results. The systematic uncertainties of our calculated fluxes are not known but are probably of the order of 10–20% and possibly greater for great depths and for cases with high geomagnetic cutoff that remove most particles with energies below ~ 10 GeV.

2.4. The geomagnetic field

The magnetic field of the Earth deflects incoming cosmic-ray particles depending on their magnetic rigidity and angle of incidence. The rigidity of a cosmic-ray particle is defined as the momentum per unit charge $R = pc/Ze$, where p and Ze are the momentum and charge of the particle and c is the velocity of light. For each angle of incidence there is a "cutoff" rigidity below which the incoming particle cannot interact with the Earth's atmosphere. Values of the cutoff rigidity as a function of geographic latitude were taken from Bland and Cioni [14]. The vertical cutoff rigidity parameter ranges from zero near the geomagnetic poles to about 17.5 GV near the equator.

The value of the cutoff rigidity determines which part of the GCR particle spectrum is used for the energy distribution of incident primary particles in our calculations. The nuclear model built into the high-energy part of LCS has an upper limit on the energy of transported particles of 3.5 GeV. Applying a scaling law model, this range can be extrapolated to much higher energies. The extended model reproduces experimental data fairly well up to ~ 10 GeV. For higher energies, one has to introduce some corrections based on experimental data and simulations using the GEANT code from CERN in Geneva, which was written especially for simulations of ultra-relativistic-particle interactions with matter. These corrections increase the uncertainties (by an amount not known but probably less than $\sim 50\%$) of the particle fluxes used for regions with high geomagnetic fields that cutoff most particles with energies less than ~ 10 GeV.

We carried out the simulations of the production of in-situ cosmogenic nuclides by GCR particles with energies above 10 MeV. This energy corresponds to the production at locations with high geomagnetic latitudes ($> 60^\circ$), where the influence of the geomagnetic field is fairly weak and negligible.

Because of the mixing processes in the atmosphere, this approach cannot be used for the study of cosmogenic nuclides in the Earth's atmosphere. To determine average worldwide production, it is necessary to integrate over the whole globe. To do this we performed simulations for nine cutoff rigidities uni-

formly distributed between 0 and 17.5 GeV and then averaged the results over the globe.

2.5. Cosmogenic-nuclide production-rate calculations

While LCS can calculate nuclide production as one of its outputs, we used this option only for the calculation of ^{14}C production by neutron-capture reactions on nitrogen, because the neutron-transport part of the MCNP code is coupled to very massive libraries that contain state-of-the-art neutron-capture cross sections. In all other cases we used LCS only to calculate the fluxes of particles that lead to cosmogenic-nuclide production. We chose this approach because we are convinced [6] that LCS is better at calculating particle fluxes than direct nuclide production, given that the measured cross sections used in particle production and transport are much more accurate than those used for the production of nuclides in the code.

The production rate of cosmogenic nuclide j at depth D in a model sphere with a radius R is

$$P_j(R, D) = \sum_i N_i \sum_k \int_0^\infty \sigma_{jik}(E_k) J_k(E_k, R, D) dE_k, \quad (1)$$

where N_i is the number of atoms for target element i per kg material in the sample, σ_{jik} is the cross section for the production of nuclide j from target element i by particles of type k with energy E_k , and $J_k(E_k, R, D)$ is the total flux of particles of type k with energy E_k at location D inside the irradiated body. As mentioned above, the particle fluxes $J_k(E_k, R, D)$ for GCR particles are calculated using LCS, and the cross sections σ_{jik} were ones evaluated by us and tested often by earlier calculations (see Section 2.7).

2.6. Production by solar protons in polar regions

The energetic particles from the Sun are $\sim 98\%$ protons and typically have energies of ~ 1 – 100 MeV, with some solar-particle events having higher energy particles [15]. Because of their relatively low energies, these solar protons only reach the Earth's atmosphere at high geomagnetic latitudes (above

about 60°). Solar protons make nuclides only in the very top of the atmosphere. The long-term average flux of solar protons is not expected to make significant amounts of cosmogenic nuclides. However, we did some calculations to check this expectation. Also, some huge solar-particle events have proton fluxes much higher than average, such as those in October 1989 [16], and such huge solar-particle events could make a contribution to the cosmogenic nuclides found in some layers in polar ice, such as in Greenland and Antarctica.

The production rates of cosmogenic nuclides by solar protons in the atmosphere above the Earth's poles were calculated with the model developed for the Moon by Reedy and Arnold [5]. This model considers only the slowing and stopping of solar protons by ionization energy losses. A typical solar proton has an energy of only about 30 MeV, which has a range in the atmosphere of only about 1 g cm^{-2} , and most protons are stopped before they induce a nuclear reaction. The uncertainties in these rates for SCR-produced nuclides are dominated by uncertainties in the incident particle fluxes as the cross sections for these reactions are fairly well known.

We used the fluxes and energy spectra both for the long-term average determined for solar protons and for the October 1989 solar particle events. The long-term-averaged integral flux of solar protons above $10 \sim \text{MeV}$, determined from nuclides in the tops of lunar rocks, was taken to be $70 \text{ protons cm}^{-2} \text{ s}^{-1}$ with an exponential-rigidity spectral shape of $R_0 = 75 \text{ MV}$ [17]. Different nuclides give different fluxes for this long-term averaged SCR flux, and the uncertainty for the long-term rates for production by SCR particles is estimated to be of the order of 30%. For the energetic protons during October 1989, we averaged their omnidirectional fluence (4.2×10^9 and $1.9 \times 10^{10} \text{ protons cm}^{-2}$ above 30 and 10 MeV, respectively [16]) over a year (a typical atmospheric residence time for most cosmogenic nuclides) and used an exponential-rigidity spectral shape with $R_0 = 68 \text{ MV}$. Note that the solar protons during October 1989 were very intense, more than some complete 11-year solar cycles [16], and among the biggest in many decades [8,15]. The production rates by solar-protons were calculated with Eq. 1 using the proton fluxes calculated using the slowing-down

model [5] and cross sections for proton-induced reactions.

2.7. Cross sections for cosmogenic-nuclide production by spallation reactions

For production in surface rocks, the cross sections for the production of cosmogenic nuclides by GCR particles (almost entirely neutrons) were those well tested for extraterrestrial samples (e.g., [6,7]). We only considered the main terrestrial minerals of interest to date, quartz, calcite, and those common in basalts (such as olivine), with the main target elements of interest being O, Mg, Si, Ca, and Fe. We have generally been able to reproduce measured cosmogenic-nuclide production rates in extraterrestrial matter to within $\sim 10\%$.

For the Earth's atmosphere, cross sections for oxygen were those used for extraterrestrial matter (e.g., [6,7]). As we have done little work with targets of nitrogen and argon, we had to find and often estimate cross sections for these important atmospheric targets. For the production of ^3H , the cross sections of [18] were used.

For the $\text{N}(\text{p},\text{x})^7\text{Be}$ and $\text{N}(\text{p},\text{x})^{10}\text{Be}$ reactions, the cross sections used were based on measurements (mainly [19–21]). The cross sections for ^7Be from nitrogen are fairly large because the main reaction is $^{14}\text{N}(\text{p},2\alpha)^7\text{Be}$, with a threshold energy of 10.5 MeV. The cross sections for the $\text{N}(\text{n},\text{x})^7\text{Be}$ reactions were those for the (p,x) reaction above 300 MeV but dropping rapidly to zero at a neutron energy of 42 MeV. The cross sections for the $\text{N}(\text{n},\text{x})^{10}\text{Be}$ reaction are the (p,x) values above 600 MeV and measurements for neutron energies below 35 MeV [22], which are fairly large for the $^{14}\text{N}(\text{n},\text{p}\alpha)^{10}\text{Be}$ reaction with a threshold energy of only 11.4 MeV.

Unpublished cross sections [D. Huggle, Y. Parrat, and E. Nolte, pers. commun., 1994, and papers in prep.] were used for the $\text{Ar}(\text{p},\text{x})^{36}\text{Cl}$ reaction, which below about 40 MeV is mainly the $^{40}\text{Ar}(\text{p},\alpha\text{n})^{36}\text{Cl}$ reaction with a threshold of only 7.2 MeV. The cross sections for the $^{40}\text{Ar}(\text{n},\text{p}4\text{n})^{36}\text{Cl}$ reaction were assumed the same as the $^{40}\text{Ar}(\text{p},2\text{p}3\text{n})^{36}\text{Cl}$ ones above about 80 MeV and dropping to zero at 40 MeV. Cross sections for the $^{36}\text{Ar}(\text{n},\text{p})^{36}\text{Cl}$ reaction were estimated from cross sections for similar reactions.

These cross sections for nitrogen and argon have not been tested like the cross sections used for surface materials, so it is hard to assign uncertainties to them. The cross sections for proton-induced reactions are probably about as good as the uncertainties in their measurements, usually about 10–20%. The reported uncertainties for the $\text{N}(\text{n},\text{x})^{10}\text{Be}$ reaction [22] are about 25%. The uncertainties in the other neutron-induced cross sections are unknown, but probably of the order of 25–50%. The best reactions for making these atmospheric cosmogenic nuclides are protons on Ar for ^{36}Cl and on N for ^7Be (although fluxes of GCR protons tend to be low) and neutrons (GCR secondaries) on N for ^{10}Be .

3. Results and discussion

3.1. Neutron fluxes

The principal feature of the depth dependence of the total neutron flux is the maximum in the altitude range corresponding to a depth 75–125 g cm^{-2} . This maximum occurs at all latitudes and arises from the depletion of the neutron density at high altitudes by neutron leakage out of the atmosphere. At depths in the atmosphere exceeding $\sim 150 \text{ g cm}^{-2}$, the total flux shows primarily an exponential dependence with an effective attenuation length that varies from about 178 g cm^{-2} near the equator to 158 g cm^{-2} near the poles. For depths greater than $\sim 150 \text{ g cm}^{-2}$, the shape of the neutron energy spectrum changes very slowly with depth. The latitude variations of the incident primary cosmic-ray intensity are similarly reflected in the variations of total-neutron flux magnitude. Because neutron multiplicity is approximately a logarithmic function of interaction energy, the variations with geomagnetic latitude in the magnitude of the total neutron flux are somewhat smaller than those for the incident GCR flux.

This exponential dependence of the neutron flux with atmospheric depth is disturbed only near the air-surface interface, where the total neutron flux shows considerable variation (Fig. 1). This variation is caused mainly by differences in production and transport processes in these two materials and by the reflection of neutrons by the surface back into the air

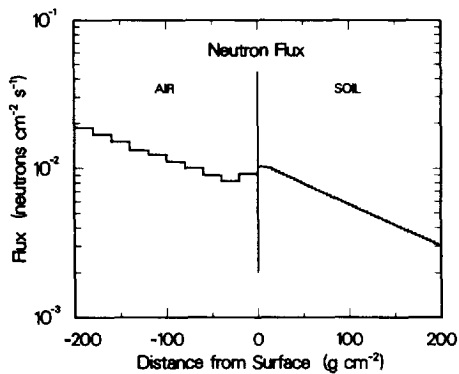


Fig. 1. The calculated total flux of neutrons on either side of the air–surface interface, which shows boundary effects for ~ 10 – 20 g cm^{-2} on both sides of this boundary.

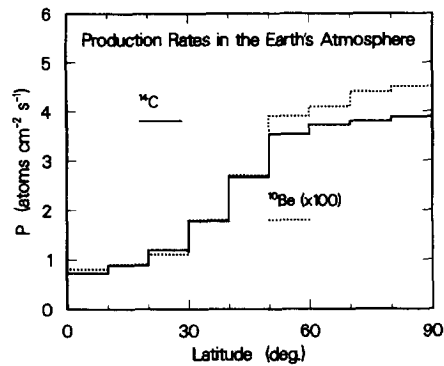


Fig. 2. The calculated production rate of cosmogenic ^{14}C and ^{10}Be (multiplied by 100) in the Earth's atmosphere as a function of geomagnetic latitude.

(cf., [23]). The shape of this variation is dependent upon the assumed elemental composition of the surface [23]. For example, the addition of water to the surface would have a significant effect on the thermal-neutron flux because of the large thermal-neutron absorption and scattering cross sections of hydrogen.

3.2. Production of cosmogenic nuclides in the Earth's atmosphere

The production rates of cosmogenic nuclides have latitude and altitude dependences that reflect those for the fluxes of the primary and secondary cosmic-

ray particles. The total production rates for all calculated nuclides were obtained by adding the contributions from reactions initiated by nucleons on all possible target elements as a function of altitude at 10° latitude intervals. Integration over latitude and altitude yields a global average production rate of the investigated cosmogenic nuclide.

As the most investigated cosmogenic nuclide produced in the Earth's atmosphere is ^{14}C , we give some details about the calculation of its production rate with our model. ^{14}C is produced in the atmosphere by a variety of nuclear reactions, but the contribution of the $^{14}\text{N}(n,p)^{14}\text{C}$ reaction is orders of magnitude greater than other reactions. Using calcu-

Table 1
Calculated production rates of cosmogenic nuclides in the Earth's atmosphere, globally averaged for GCR particles and for polar regions (geomagnetic latitudes above $\sim 60^\circ$) for solar protons (SCR). The flux used for the solar protons in October 1989 was the number of protons in the 19–30 October 1989 solar-particle events divided by one year

Nuclide	Half-life (years)	Production rates ($\text{atoms cm}^{-2} \text{s}^{-1}$)		
		GCR	Avg. SCR	SCR (Oct. 1989)
^3H	12.3	0.26	4.3×10^{-3}	0.018
^7Be	0.147	0.0129	0.0134	0.068
^{10}Be	1.5×10^6	0.0201	1.8×10^{-4}	6.2×10^{-4}
^{14}C	5730	1.91	3.2×10^{-4}	1.5×10^{-3}
^{36}Cl	3.0×10^5	1.18×10^{-3}	2.1×10^{-4}	1.0×10^{-3}

lated fast neutron and proton fluxes, we found that the contribution to the ^{14}C production from spallation of oxygen is about 0.7%. The calculated dependence of ^{14}C production rate on geomagnetic latitude is shown in Fig. 2. For the purpose of these calculations, both polar and equatorial symmetry in geomagnetic coordinates are assumed. We calculated a mean production rate of ^{14}C of 1.85×10^{-3} atoms $\text{g}^{-1} \text{s}^{-1}$ in the Earth's atmosphere. The depth profile for the production of ^{14}C is similar to that for neutron fluxes. Since the Earth's atmosphere is 1033 g cm^{-2} thick, the global average production rate of ^{14}C is $1.91 \text{ atoms cm}^{-2} \text{s}^{-1}$, with an uncertainty of $\sim 20\%$ due mainly to the uncertainties in the fluxes, especially at low geomagnetic latitudes (as the cross sections are well measured). This value is in good agreement with estimates of the radiocarbon production rate based on analysis of the specific activity of ^{14}C (e.g., $1.99 \text{ atoms cm}^{-2} \text{s}^{-1}$ [24]) and with other theoretical predictions (e.g., 1.8 [4], 1.75 [25], and $1.89 \text{ atoms cm}^{-2} \text{s}^{-1}$ [26]).

The calculated dependence on geomagnetic latitude of the ^{10}Be production rate (spallation reactions on nitrogen and oxygen) is shown in Fig. 2 and is fairly similar to that for ^{14}C . The uncertainty in our calculated ^{10}Be production rates are $\sim 30\%$ near the poles (due to uncertainties in both particle fluxes and cross sections) and probably $\sim 50\%$ near the equator (higher due to greater uncertainties in fluxes for regions of high geomagnetic cutoffs). Uncertainties for other GCR-produced nuclides are higher due to greater uncertainties in their production cross sections. Table 1 summarizes the results of our calculations of globally-averaged production rates for all investigated atmospheric cosmogenic nuclides by GCR particles, the long-term average flux of solar protons, and the number of solar protons in October 1989 divided by one year. The values for nuclides with half-lives longer than about 1 solar cycle represent the total amount actually present in the environment. The concentrations in the Earth's atmosphere of nuclides with short lifetimes vary with the amount of solar activity (see below), and the given values represent only long-term averages.

The GCR production rates of the nuclides made by spallation reactions in the atmosphere (all the radionuclides except ^{14}C) were previously not well determined, especially experimentally. For ^{10}Be , our

calculated production rate of $0.0201 \text{ atoms cm}^{-2} \text{s}^{-1}$ is close to that estimated from measurements of ocean cores, $0.026 \text{ atoms cm}^{-2} \text{s}^{-1}$ [21], but lower than that determined from ^{10}Be measured in precipitation, $0.038 \pm 0.008 \text{ atoms cm}^{-2} \text{s}^{-1}$ [27].

Our calculated production rate of ^3H of $0.26 \text{ atoms cm}^{-2} \text{s}^{-1}$ agrees fairly well with those calculated by Nir et al. [18], whose ^3H rate was $0.19 \text{ atoms cm}^{-2} \text{s}^{-1}$, and by O'Brien et al., whose calculated rates were $0.255 \text{ atoms cm}^{-2} \text{s}^{-1}$ [25] and $0.285 \text{ atoms cm}^{-2} \text{s}^{-1}$ [26]. For the other three spallogenic radionuclides, our calculated rates and those in O'Brien et al. [26] (which are 1.135 times those in [25]) are, respectively, 0.0129 and $0.0631 \text{ atoms cm}^{-2} \text{s}^{-1}$ for ^7Be , 0.0201 and $0.0285 \text{ atoms cm}^{-2} \text{s}^{-1}$ for ^{10}Be , and 1.18×10^{-3} and $9.83 \times 10^{-4} \text{ atoms cm}^{-2} \text{s}^{-1}$ for ^{36}Cl . The reason for the large (factor of ~ 5) difference in our production rate for ^7Be and that of [26] is not known but probably is in the cross sections used for the $^{14}\text{N}(n,x)^7\text{Be}$ reaction. Our calculated production rate for ^{10}Be agrees well with that of [21], $0.021(\pm 0.005) \text{ atoms cm}^{-2} \text{s}^{-1}$.

Ratios of these radionuclides have been measured in some samples, although it is not clear that such measured ratios represent production ratios in the atmosphere (for example, such ratios vary widely in precipitation, e.g., [28]). Our calculated GCR production ratios for $^7\text{Be}/^{36}\text{Cl}$ and $^{10}\text{Be}/^{36}\text{Cl}$ are 11 and 17, respectively. Measured $^7\text{Be}/^{36}\text{Cl}$ and $^{10}\text{Be}/^{36}\text{Cl}$ ratios in precipitation scatter about 10 [28], and the mean measured $^{10}\text{Be}/^{36}\text{Cl}$ ratio in ice cores from Camp Century in Greenland is about 8 [29]. The $^{10}\text{Be}/^7\text{Be}$ production ratio is very important for studies of atmospheric processes [30]. Our calculated global $^{10}\text{Be}/^7\text{Be}$ production ratio for GCR particles is about 1.6, similar to or lower than this ratio measured in samples collected at times of low solar-proton fluxes [30] but much higher than an estimated production ratio of about 0.5 [30].

For ^3H , ^{10}Be , and ^{14}C , the calculated production rates by solar protons (SCR particles) in Table 1 for polar regions are about a percent or less of the GCR rates. However, the long-term averaged calculated SCR/GCR production ratios near the poles are 1.04 for ^7Be and 0.18 for ^{36}Cl . These high ratios can be understood by the cross sections for the production of these two radionuclides by GCR neutrons and by

protons, as both radionuclides have high cross sections at low energies for protons and low cross sections at much higher energies for neutrons. However, production by solar protons only occurs for regions of the Earth where the geomagnetic cutoffs are less than about 10 MeV, which is a fairly small fraction (~ 0.1 – 0.2) of the total area of the Earth. Large solar particle events are rare [8,15,16], and the polar SCR/GCR production ratios for most years will be lower than these averaged ratios. The calculated production rates for a year with intense solar particle events, the October 1989 column in Table 1, are about a factor of 4–5 higher than the rates for the long-term averaged SCR fluxes, and solar-proton production of ^7Be and possibly ^{36}Cl could be important in years with intense solar particle events, especially for large events with relatively more high-energy protons than the October 1989 events. Movement of solar-proton-produced radionuclides from the polar regions or out of the atmosphere could affect measured amounts of ^7Be and ^{36}Cl .

3.3. Production of cosmogenic nuclides in the Earth's surface

Having calculated fluxes of particles in the Earth's surface, we calculated production rates of cosmogenic nuclides using Eq. 1. In the interactions of primary cosmic-ray particles with the Earth's atmosphere and during the development of particle cascades, particle fluxes undergo a continuous change in the sense of the spectral shape of their distribution and relative ratios of various particles. From the point of view of cosmogenic-nuclide production in the outermost few g cm^{-2} of Earth's atmosphere, the most important particles are protons and neutrons. Going deeper into the atmosphere, the proton fluxes decrease faster than the neutron fluxes, and therefore neutrons become even more dominant for cosmogenic-nuclide production. At sea level the muon fluxes start to become significant.

There are three principal mechanisms by which the cosmogenic nuclides can be produced in the

Table 2
Calculated and measured production rates of cosmogenic nuclides at the Earth's surface at sea level (atmospheric thickness of 1033 g cm^{-2}) with no geomagnetic cutoff and calculated and measured e-folding lengths (L_e) below the surface ([35–47])

Nuclide	Target	Production rate atoms yr^{-1} (g-target) $^{-1}$		L_e g cm^{-2}	
		Calc. ^a	Measured	Calc. ^a	Measured
^3He	SiO_2	124.		158	
^{10}Be	SiO_2	5.97	6.0 [35,36], 6.4 [37]	157	145 [38], 159 ^b
^{14}C	SiO_2	18.6	20 [39]	162	
^{21}Ne	SiO_2	18.4	21 [40]	167	179 ^b
^{26}Al	SiO_2	36.1	36.8 [35,36], 41.7 [37]	158	156 [38], 166 ^b
^{36}Cl	CaO	46.2	54 [41], 52 [42]	158	
^3He	basalt ^c	105.	107 ^d [43], 109 [44], 115 [45]	158	159 [46], 165 [47]
^{21}Ne	basalt ^c	41.1	45 [44]	167	165.5 [46]

^a Does not include any muon contributions.

^b K. Nishiizumi, J. Poths et al., pers. commun., 1993.

^c Calculations done for Fo_{81} olivine (41.9% O, 25.8% Mg, 18.4% Si, and 13.9% Fe).

^d From the reported value of 97 for 37°N geomagnetic latitude using the geomagnetic latitude correction factors of [1].

Earth's surface: (a) by spallation of target nuclei by energetic nucleons, (b) by neutron-capture reactions, and (c) by muon-induced nuclear reactions. The production rates presented below are only for spallation reactions calculated on the basis of neutron and proton fluxes in the Earth's surface. Examples of production rates of nuclides produced by neutron-capture reactions are reported in Dep et al. [31], and further investigation is in progress. We did not calculate the contribution to the total production rates of cosmogenic nuclides from muon-induced reactions because of the lack of the data needed to convert muon intensities to production rates (such as yields per capture of stopped negative muons). This contribution was estimated to be relatively low (less than $\sim 10\%$) at the Earth's surface, but it increases as one goes to larger depths [1].

As shown in Fig. 1, the depth dependence of neutron flux shows a relatively flat profile near the surface–air interface to a depth of about 12 g cm^{-2} and then decreases roughly exponentially with increasing depth. As the spectral shapes of differential neutron and proton fluxes change very little with increasing depth below the Earth's surface, a similar depth dependence is expected also for the production rate profile.

Ignoring this surface–air interface region, the production rate $P(x)$ of a cosmogenic nuclide at a depth x (cm) can be expressed as $P(x) = P(0)e^{-(\rho x/L_e)}$, where $P(0)$ is the production rate of the cosmogenic nuclide at the Earth's surface, ρ is the density of the Earth's surface, and L_e is the length (in g cm^{-2}) that the nuclide's production rate decreases by $1/e$ with depth in the Earth's surface. The surface production rates were calculated with our model, and the e-folding lengths were determined from the production-rate depth profiles. Calculated production rates and e-folding lengths are given in Table 2 for geomagnetic latitudes above about 60° . The general shapes of all calculated depth profiles are very similar, and therefore only one example (the ^{10}Be depth profile) is given in Fig. 3. All other depth profiles can be reproduced using the calculated surface production rates and e-folding lengths (Table 2).

In Table 2, our calculated production rates for production by energetic neutrons and protons at sea level and for no geomagnetic cutoff agree well with the measured values. The uncertainties in our calcu-

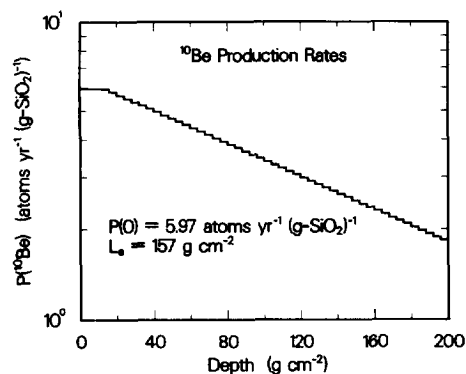


Fig. 3. The calculated production rate of ^{10}Be as a function of depth in the Earth's surface at sea level for high geomagnetic latitudes using an effective incident proton flux of $4.56 \text{ protons cm}^{-2} \text{ s}^{-1}$ above 10 MeV. The surface production rate ($P(0)$) and the e-folding length with depth (L_e) are indicated.

lated production rates are probably a little greater than those for these nuclides in extraterrestrial matter because our codes have not been tested for such great depths and are estimated to be $\sim 20\%$. This uncertainty does not include any contribution for the omission of muon production, which is an unknown but probably small ($< 10\%$) contribution at the very surface of the Earth. Our calculated production rates tend to be low, which could be partially because we have omitted production by muons. The fraction of muon production at the surface is not well known, but we would estimate that this fraction is low given the good agreement of our calculated production rates and of our calculated e-folding lengths with the measured ones. As muons have much longer e-folding lengths [1], a significant fraction of the production at the surface by muons would have resulted in measured e-folding lengths much greater than those due just to neutrons and protons, although most measurements were made at high altitudes where muons contributions are less than at sea level.

Our calculated in-situ production rates generally differ significantly with those calculated by Yokoyama et al. [32]. For example, our calculated $^{26}\text{Al}/^{10}\text{Be}$ production ratio in quartz is 5.7, while their value is 17.4 [32]. Detailed comparisons with their absolute rates are complicated by our having different factors for changes with altitude than theirs (because their adopted attenuation length is longer than those used by most others), but many of the

calculated production-rate differences are of the order of a factor of 2. The cross sections that we used, especially for ^{10}Be , and the different nature of the models for the fluxes of cosmic-ray particles, could account for these big differences.

The production rates for in situ nuclides reported by Lal [33] for ^{10}Be , ^{26}Al , and ^{14}C were normalized to experimental values and agree very well with our calculated rates. His calculated elemental production rates for ^3He and ^{21}Ne , respectively, gives rates in quartz of 75 and 9.6 atoms $\text{yr}^{-1} (\text{g-SiO}_2)^{-1}$ (versus our rates of 124 and 18.4 atoms $\text{yr}^{-1} (\text{g-SiO}_2)^{-1}$, respectively) and rates in Fo_{81} olivine of 64 and 32 atoms $\text{yr}^{-1} (\text{g-SiO}_2)^{-1}$ (versus our rates of 105 and 41.1 atoms $\text{yr}^{-1} (\text{g-SiO}_2)^{-1}$, respectively). As noted by Lal [33] for his ^3He , neon, and argon production rates, “(t)hese estimates must be considered tentative since they are largely based on proton excitation functions; here also the data are limited.” Differences in cross sections could easily explain most of these differences.

To investigate the influence of altitude on cosmogenic-nuclide production, we calculated production rates in the Earth’s surface near the poles at altitudes from 0 to 5 km above the sea level. Results for the investigated nuclides are shown in Fig. 4. All nuclides show the same dependence of production rate on altitude. With an increase in altitude, the production rate increases approximately exponentially, in agreement with the observed dependence of total

particle flux on altitude. Relative to sea level, our calculated production rates at 3-km and 5-km altitude are factors of ≈ 9.5 and ≈ 28 times higher, respectively, versus factors of 10 and 30 for Lal [1] and about 7 and 20 for Yokoyama et al. [32] for these altitudes. As noted above, Yokoyama et al. [32] adopted an attenuation length (192 g cm^{-2}) that is longer than those used by others. The production rate as a function of altitude is not a simple function, but up to about 4 km all of our calculated production rates increase roughly exponential with altitude with an e-folding length of about 1.4 km. Neutron contributions to the total production rates range from $\approx 95\%$ at sea level to $\approx 93\%$ at 5 km above the sea level.

3.4. Geomagnetic effects

The production rates of these cosmogenic nuclides are affected by the strength of the Earth’s magnetic field at a given location. The magnitude of this effect with geomagnetic latitude for the present field strength is shown in Fig. 2 for atmospheric ^{14}C and ^{10}Be . Our calculated variations with geomagnetic latitude is similar to but a little greater than that of [1] at altitudes of 10 km and less. However, as noted above, our codes have not been tested for high magnetic fields that cutoff GCR particles with energies above $\sim 10 \text{ GeV}$. The fairly good agreement of our global atmospheric production rates with those of others indicate that our codes are not bad for the cases with high magnetic fields, but we do not have enough confidence yet to assign low uncertainties to our production rates for locations with high magnetic fields. We only have confidence for the regions of very low magnetic fields, conditions that also apply to all meteorites and lunar samples. For the polar regions of the Earth, we would estimate our uncertainties to be $\sim 20\%$ for nuclides with well measured or tested cross sections (^{14}C and ^{10}Be) and probably higher (by unknown amounts) for other nuclides. For near-equatorial regions, our uncertainties are unknown but are much greater than for polar regions.

For the nuclides made in situ in the Earth’s surface, we have even less confidence in calculating variations in production rates with geomagnetic field.

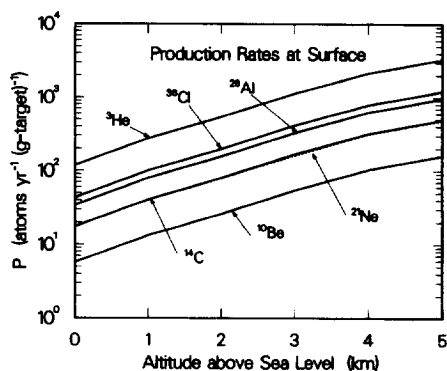


Fig. 4. The calculated production rates of in-situ cosmogenic nuclides as a function of altitude for high geomagnetic latitudes using an effective incident proton flux of $4.56 \text{ protons cm}^{-2} \text{ s}^{-1}$ above 10 MeV. The target for ^{36}Cl is CaO and for the other nuclides is SiO_2 .

For in situ ^{10}Be at sea level, we calculated that the production rate near the geomagnetic equator is down from that near the poles by a factor of about 3.2, which is much more than that (1.8) in [1]. This production-rate variation for in situ ^{10}Be at sea level is less than our calculated variation in atmospheric ^{10}Be with geomagnetic latitude, which is about a factor of 5.6.

Globally-averaged production rates can vary much with major changes in the strength of the Earth's magnetic field [25,26]. We did not model variations in production rates for periods when the Earth's global magnetic field strength was different that it is today. Recent variations in the Earth's magnetic field is a factor that can affect production rates determined from measured concentrations of these nuclides (e.g., [34]). Such geomagnetic variations would have very little effect on production rates near the magnetic poles, the calculations that we have the most confidence on. For periods of very low geomagnetic fields, our polar calculations would apply to most of the Earth, and both GCR and especially SCR global production rates would be much higher than they are now.

3.5. Solar-cycle effects

Another complication for the calculation of realistic production rates is that all production rates depend on the incident flux of GCR particles in the inner solar system, which in turn depends on the nature of solar activity. For GCR particles, this variation over a solar cycle is included in the primary GCR spectrum through the modulation parameter ϕ . Since one does not know a priori the amount of solar modulation, the dependence of production rates on solar modulation was investigated. We performed calculations of GCR particle fluxes and cosmogenic-nuclide production rates for primary spectra with modulation parameters ϕ of 375 and 950 MeV. For atmospheric cosmogenic nuclides, the fluxes of solar protons near the poles can vary greatly with time and the phase of the solar cycle. Near the geomagnetic equator with the Earth's current magnetic fields, the effects of solar modulation is much less as cosmic-ray particles with energies above ~ 10 GeV are not affected much by solar modulation.

The calculations that we did for the fluxes of GCR particles at the minimum in solar activity (the time of the highest fluxes of GCR particles), $\phi = 375$ MeV, and solar maximum, $\phi = 950$ MeV, indicate that production rates vary by factors of about 2.4 over a typical 11-year solar cycle, in agreement with earlier calculations of such effects [12]. At the poles, the variation in the production rates of atmospheric cosmogenic nuclides is about 2.5, with the global variation for these nuclides being 2.4. The global production rates for atmospheric cosmogenic nuclides at solar minimum are about 1.49 times those for the GCR flux averaged over a complete solar cycle, and the rates at solar maximum are 0.62 times the average rates. For in-situ terrestrial cosmogenic nuclides, the ratios for solar minimum and maximum to the average GCR rate are 1.49 and 0.63, respectively. We did not calculate production rates for periods of very low solar activity (values of ϕ near 0), but earlier calculations of Reedy [12] indicate that production rates for regions with no geomagnetic fields could be higher than for average solar activity ($\phi = 550$ MeV) by factors of ~ 2 –5 for periods of very low solar activity.

These variations in production rates of atmospheric cosmogenic nuclides do not consider any contributions from solar protons, which are present irregularly [8,15,16] (although almost never present for about 4 years around solar minimum) in the polar regions and only produce nuclides within $\sim 30^\circ$ of the geomagnetic poles. The solar-proton calculations using the proton fluxes for October 1989 should be representative of the largest production rates by solar protons, with the minimum rates being essentially zero for the many long time periods when solar proton fluxes are very low [8,15,16].

4. Conclusions

A purely physical Monte Carlo model was used for the investigation of the production and transport of galactic-cosmic-ray particles in the Earth's atmosphere and surface. This model enables us to calculate differential particle fluxes as a function of altitude, chemical composition, and geomagnetic latitude for a variety of initial irradiation conditions.

The calculated particle fluxes have been used for the calculation of cosmogenic-nuclide production rates in the Earth's atmosphere and surface. Reactions of solar protons with the atmosphere over polar regions were also investigated.

The calculated production rate of radiocarbon (^{14}C) in the Earth's atmosphere ($1.91 \text{ atoms cm}^{-2} \text{ s}^{-1}$) agree well with measured and other calculated values. Our calculated production rates for ^3H , ^{10}Be , and ^{36}Cl are not in bad agreement with most previous calculations, but our rate for making atmospheric ^7Be is much lower than those in previous calculations, probably because of the cross sections used for the reactions making ^7Be . The production in polar regions of these atmospheric cosmogenic nuclides by solar protons is unimportant except for ^7Be and, to a lesser extent, ^{36}Cl , both which could be made in significant amounts during times of very high solar-proton fluxes.

The calculated GCR production rates by neutrons and protons at the surface of the Earth for high geomagnetic latitudes for ^3He , ^{10}Be , ^{14}C , ^{21}Ne , ^{26}Al , and ^{36}Cl agree well with measured rates. All calculated production rates for in-situ nuclides made by energetic nucleons decrease exponentially with depth with e-folding lengths of $\approx 157\text{--}167 \text{ g cm}^{-2}$, again in good agreement with measured values. The production rates increase approximately exponentially with the increase of altitude. The production rates at 3-km altitude are ≈ 9.5 times higher than at sea level, versus the factors of 10 given by Lal [1] and 7 by Yokoyama et al. [32]. The neutron contribution to the total production rates by nucleons is higher than $\approx 93\%$.

These agreements for terrestrial GCR-produced nuclides and similar results for extraterrestrial objects show that our model based on LCS can be used to obtain good GCR production rates of terrestrial cosmogenic nuclides, especially for regions of low geomagnetic fields, and they show that our model should be good for very deep in extraterrestrial objects, including those with atmospheres. However, for many applications, it is necessary to improve the calculations in the sense of the extension of the nuclear model used for particle–nucleus interaction to higher energies (above 10 GeV). This extension is necessary for accurate simulation of production rates at lower geomagnetic latitudes, where many particles

are prevented from interacting with the Earth by the geomagnetic field.

Acknowledgements

We thank K. Nishiizumi, D. Lal, D. Fink, C. Tuniz, T. Cerling, M. Imamura, D. Elmore, P. Kubik, E. Nolte, and many other colleagues for their encouragement in doing this work and for some of the data used in this work. We thank J. Beer, J. Gosse, F. Phillips, D. Elmore, M. Kurz, K. Nishiizumi, and M. Kastner for their good comments. We especially appreciate the constructive comments by R. Byrd that greatly helped this manuscript. This work was supported in part by NASA and was done under the auspices of the U.S. Department of Energy. [MK]

References

- [1] D. Lal, In situ-produced cosmogenic isotopes in terrestrial rocks, *Annu. Rev. Earth Planet. Sci.* 16, 355–358, 1988.
- [2] T.E. Cerling and H. Craig, Geomorphology and in-situ cosmogenic nuclides, *Annu. Rev. Earth Planet. Sci.* 22, 273–317, 1994.
- [3] R.C. Reedy, C. Tuniz and D. Fink, Report on the workshop on production rates of terrestrial in-situ-produced cosmogenic nuclides, *Nucl. Instrum. Methods B92*, 335–339, 1994.
- [4] D. Lal and B. Peters, Cosmic ray produced radioactivity on the Earth, in: *Handbuch der Physik*, XLVI/2, Springer, Berlin, pp. 551–612, 1967.
- [5] R.C. Reedy and J.R. Arnold, Interaction of solar and galactic cosmic-ray particles with the Moon, *J. Geophys. Res.* 77, 537–555, 1972.
- [6] J. Masarik and R.C. Reedy, Effects of bulk chemical composition on nuclide production processes in meteorites, *Geochim. Cosmochim. Acta* 58, 5307–5317, 1994.
- [7] R.C. Reedy and J. Masarik, Cosmogenic-nuclide depth profiles in the lunar surface, *Lunar Planet. Sci.* 25, 1119–1120, 1994.
- [8] R.C. Reedy, Solar proton fluxes since 1956, *Proc. Lunar Sci. Conf.* 8th, 825–839, 1977.
- [9] R.E. Prael and H. Lichtenstein, User guide to LCS: The LAHET Code System, Los Alamos Natl. Labor. rep., LA-UR-89-3014, 76 pp., 1989.
- [10] J.F. Briesmeister, MCNP—A general Monte Carlo N-particle transport code, version 4A, Los Alamos Natl. Labor. rep., LA-12625-M, 693 pp., 1993.
- [11] G.C. Castagnoli and D. Lal, Solar modulation effects in terrestrial production of carbon 14, *Radiocarbon* 22, 133–158, 1980.

- [12] R.C. Reedy, Nuclide production by primary cosmic-ray protons, *Proc. Lunar Planet. Sci. Conf.* 17th, in: *J. Geophys. Res.* 92, E697–E702, 1987.
- [13] K.S.W. Champion, A.E. Cole and A.J. Kantor, Standard and reference atmospheres, in: *Handbook of Geophysics and the Space Environment*, A.S. Jursa, ed., pp. 14-1–14-43, Air Force Geophys. Labor., U.S. Air Force, 1985.
- [14] C.J. Bland and C. Cioni, Geomagnetic cutoffs rigidity in non-vertical directions, *Earth Planet. Sci. Lett.* 4, 399–405, 1968.
- [15] D.F. Smart and M.A. Shea, Solar proton events during the last three solar cycles, *J. Spacecraft Rockets* 26, 403–415, 1989.
- [16] M.A. Shea and D.F. Smart, Recent and historical solar proton events, *Radiocarbon* 34, 255–262, 1992.
- [17] M.N. Rao, D.H. Garrison, D.D. Bogard and R.C. Reedy, Determination of the flux and energy distribution of energetic solar protons in the past 2 Myr using lunar rock 68815, *Geochim. Cosmochim. Acta* 58, 4231–4245, 1994.
- [18] A. Nir, S.T. Kruger, R.E. Lingenfelter and E.J. Flamm, Natural tritium, *Rev. Geophys.* 4, 441–456, 1966.
- [19] R. Bodemann, H.-J. Lange, I. Leya, R. Michel, T. Schiekel, R. Rösel, U. Herpers, H.J. Hofmann, B. Dittrich, M. Suter, W. Wölfli, B. Holmqvist, H. Condé and P. Malmberg, Production of residual nuclei by proton-induced reactions on C, N, O, Mg, Al and Si, *Nucl. Instrum. Methods B82*, 9–31, 1993.
- [20] G.M. Raisbeck and F. Yiou, The application of nuclear cross section measurements to spallation reactions in cosmic rays, in: *Spallation Nuclear Reactions and Their Applications*, B.S.P. Shen and M. Merker, eds., pp. 83–111, Reidel, Dordrecht, 1976.
- [21] J.-L. Reyss, Y. Yokoyama and F. Guichard, Production cross sections of ^{26}Al , ^{22}Na , ^7Be from argon and of ^{10}Be , ^7Be from nitrogen: Implications for production rates of ^{26}Al and ^{10}Be in the atmosphere, *Earth Planet. Sci. Lett.* 53, 203–210, 1981.
- [22] T. Nakamura, H. Sugita, M. Imamura, Y. Uwamino, S. Shibata, H. Nagai, M. Takebatake and K. Kobayashi, Measurement of long-lived ^{10}Be , ^{14}C , and ^{26}Al production cross sections for 10–40 MeV neutrons by accelerator mass spectrometry, in: *Nuclear Data for Science and Technology*, S.M. Qaim, ed., pp. 714–716, Springer, Berlin, 1992.
- [23] K. O'Brien, H.A. Sandmeier, G.E. Hansen and J.E. Campbell, Cosmic ray induced neutron background sources and fluxes for geometries of air over water, ground, iron, and aluminum, *J. Geophys. Res.* 83, 114–120, 1978.
- [24] P.E. Damon, J.C. Lerman and A. Long, Temporal fluctuations of atmospheric ^{14}C : causal factors and implications, *Annu. Rev. Earth Planet. Sci.* 6, 457–494, 1978.
- [25] K. O'Brien, Secular variations in the production of cosmogenic isotopes in the Earth's atmosphere, *J. Geophys. Res.* 84, 423–431, 1979.
- [26] K. O'Brien, A. de la Zerda Lerner, M.A. Shea and D.F. Smart, The production of cosmogenic isotopes in the Earth's atmosphere and their inventories, in: *The Sun in Time*, C.P. Sonett, M.S. Giampapa, and M.S. Matthews, eds., pp. 317–342, Univ. Arizona Press, Tucson, 1991.
- [27] M.C. Monaghan, S. Krishnaswami and K.K. Turekian, The global-average production rate of ^{10}Be , *Earth Planet. Sci. Lett.* 76, 279–287, 1985/86.
- [28] D.L. Knies, D. Elmore, P. Sharma, S. Vogt, R. Li, M.E. Lipschutz, G. Petty, J. Farrell, M.C. Monaghan, S. Fritz and E. Agee, ^7Be , ^{10}Be , and ^{36}Cl in precipitation, *Nucl. Instrum. Methods B92*, 340–344, 1994.
- [29] N.J. Conrad, P.W. Kubik, H.E. Gove and D. Elmore, A ^{36}Cl profile in Greenland ice from AD 1265 to 1865, *Radiocarbon* 31, 585–591, 1989.
- [30] G.M. Raisbeck, F. Yiou, M. Fruneau, J.M. Loiseaux, M. Lieuvain and J.C. Ravel, Cosmogenic $^{10}\text{Be}/^7\text{Be}$ as a probe of atmospheric transport processes, *Geophys. Res. Lett.* 8, 1015–1018, 1981.
- [31] L. Dep, D. Elmore, J. Fabryka-Martin, J. Masarik and R.C. Reedy, Production rate systematics of in-situ-produced cosmogenic nuclides in terrestrial rocks: Monte Carlo approach of investigating $^{35}\text{Cl}(n,\gamma)^{36}\text{Cl}$, *Nucl. Instrum. Methods B92*, 321–325, 1994.
- [32] Y. Yokoyama, J.-L. Reyss and F. Guichard, Production of radionuclides by cosmic rays at mountain altitudes, *Earth Planet. Sci. Lett.* 36, 44–50, 1977.
- [33] D. Lal, Cosmic ray labeling of erosion surfaces: In situ nuclide production rates and erosion models, *Earth Planet. Sci. Lett.* 104, 424–439, 1991.
- [34] M.D. Kurz, D. Colodner, T.W. Trull, R.B. Moore and K. O'Brien, Cosmic ray exposure dating with in situ produced cosmogenic ^3He : results from young Hawaiian lava flows, *Earth Planet. Sci. Lett.* 97, 177–189, 1990.
- [35] K. Nishiizumi, E.L. Winterer, C.P. Kohl, J. Klein, R. Middleton, D. Lal and J.R. Arnold, Cosmic ray production rates of ^{10}Be and ^{26}Al in quartz from glacially polished rocks, *J. Geophys. Res.* 94, 17,907–17,915, 1989.
- [36] K. Nishiizumi, C.P. Kohl, J.R. Arnold, J. Klein, D. Fink and R. Middleton, Cosmic ray produced ^{10}Be and ^{26}Al in Antarctic rocks: exposure and erosion history, *Earth Planet. Sci. Lett.* 104, 440–454, 1991.
- [37] E.T. Brown, J.M. Edmond, G.M. Raisbeck, F. Yiou, M.D. Kurz and E.J. Brook, Examination of surface exposure ages of Antarctic moraines using in situ produced ^{10}Be and ^{26}Al , *Geochim. Cosmochim. Acta* 55, 2269–2283, 1991.
- [38] E.T. Brown, E.J. Brook, G.M. Raisbeck, F. Yiou and M.D. Kurz, Effective attenuation lengths of cosmic rays producing ^{10}Be and ^{26}Al in quartz: implications for exposure age dating, *Geophys. Res. Lett.* 19, 369–372, 1992.
- [39] A.J.T. Jull, N. Lifton, W.M. Phillips and J. Quade, Studies of the production rate of cosmic-ray produced ^{14}C in rock surfaces, *Nucl. Instrum. Methods B92*, 308–310, 1994.
- [40] S. Niedermann, Th. Graf, J.S. Kim, C.P. Kohl, K. Marti and K. Nishiizumi, Cosmic-ray-produced ^{21}Ne in terrestrial quartz: the neon inventory of Sierra Nevada quartz separates, *Earth Planet. Sci. Lett.* 125, 341–355, 1994.
- [41] M.G. Zreda, F.M. Phillips, D. Elmore, P.W. Kubik, P. Sharma and R.I. Dorn, Cosmogenic chlorine-36 production rates in terrestrial rocks, *Earth Planet. Sci. Lett.* 105, 94–109, 1991.
- [42] J. Stone, G.L. Allan, L.K. Fifield, J.M. Evans and A.R. Chivas, Limestone erosion measurements with cosmogenic

- chlorine-36 in calcite—preliminary results from Australia. Nucl. Instrum. Methods B92, 311–316, 1994.
- [43] M.D. Kurz, Erratum [to 47], *Geochim. Cosmochim. Acta* 51, 1019, 1987.
- [44] R.J. Poreda and T.E. Cerling, Cosmogenic neon in recent lavas from the western United States, *Geophys. Res. Lett.* 19, 1863–1866, 1992.
- [45] T.E. Cerling and H. Craig, Cosmogenic ^3He production rates from 39°N to 46°N latitude, western USA and France, *Geochim. Cosmochim. Acta* 58, 249–255, 1994.
- [46] Ph. Sarda, Th. Staudacher, C.J. Allègre and A. Lecomte, Cosmogenic neon and helium at Réunion: measurement of erosion rate, *Earth Planet. Sci. Lett.* 119, 405–417, 1993.
- [47] M.D. Kurz, In situ production of terrestrial cosmogenic helium and some applications to geochronology, *Geochim. Cosmochim. Acta* 50, 2855–2862, 1986.